

## First Principles Simulation of a Ceramic/Metal Interface with Misfit

R. Benedek,<sup>1</sup> A. Alavi,<sup>2</sup> D.N. Seidman,<sup>1</sup> L.H. Yang,<sup>3</sup> D.A. Muller,<sup>4</sup> and C. Woodward<sup>5,\*</sup>

<sup>1</sup>*Department of Materials Science and Engineering, Northwestern University, Evanston, Illinois 60208*

<sup>2</sup>*School of Mathematics and Physics, Queen's University, Belfast, BT7 1NN, Northern Ireland*

<sup>3</sup>*Condensed Matter Physics Division, Lawrence Livermore National Laboratory, Livermore, California 94551*

<sup>4</sup>*Lucent Technologies, 700 Mountain Avenue, Murray Hill, New Jersey 07974*

<sup>5</sup>*Air Force Research Laboratory, Materials and Manufacturing Directorate, Wright Patterson AFB, Dayton, Ohio 45433-7817*

(Received 12 October 1999)

The relaxed atomic structure of a model ceramic/metal interface, {222}MgO/Cu, is simulated, including lattice constant mismatch, using first principles local-density functional theory plane wave pseudo-potential methods. The 399-atom computational unit cell contains 36 O and 49 Cu atoms per layer in accordance with the 7/6 ratio of MgO to Cu lattice constants. The atomic layers on both sides of the interface warp to optimize the local bonding. The interface adhesive energy is calculated. The interface electronic structure is found to vary appreciably with the local environment.

PACS numbers: 68.35.Bs, 82.65.Dp

A fundamental understanding of ceramic/metal interfaces [1] has been elusive, despite their technological importance. Considerable recent experimental progress has been made with the measurement of the atomic structure of several model ceramic/metal interfaces, particularly by high-resolution electron microscopy (HREM) [2], Z-contrast scanning transmission electron microscopy [3], and atom-probe field ion microscopy [4]. Furthermore, spatially resolved electron-energy-loss spectroscopy (EELS) is able to elucidate the electronic structure of ceramic/metal interfaces [5]. The lack of accurate and tractable atomistic simulation methods, which would enable detailed analyses of interface atomic and electronic structures, however, impedes further progress. The disparate types of bonding on the opposite sides of the interface pose a severe obstacle to the development of compact interatomic potentials at ceramic/metal interfaces. This is particularly true for interfaces of polar character, where the atomic layers on the ceramic side of the interface are exclusively anion or cation. The implementation of interatomic potential models for nonpolar interfaces [6] may be relatively easier because the interface interactions are small compared to those in the constituent bulk metal and bulk ceramic.

First principles techniques based on local-density functional theory (LDFT) are by now routinely applied to interfaces, but almost invariably within the approximation of interface coherence, i.e., the change in the lattice constant across heterophase interfaces is neglected. The large computational effort has thus far precluded the treatment of interface misfit at the LDFT level. Interface misfit and the associated dislocation networks, however, are critical features of real ceramic/metal interfaces. In the work presented here, the misfit is included in LDFT calculations for a model interface, {222}MgO/Cu. The large lattice constant mismatch ( $a_{\text{MgO}}/a_{\text{Cu}} \approx 7/6$ ) for this interface gives rise to a relatively fine-scale misfit-dislocation network. This makes the calculation more tractable than for

systems with smaller misfit, although the calculations still require a huge computational effort on a parallel computer. The present work represents the first calculation at the first principles level of the atomic relaxation at a ceramic/metal interface with misfit [7].

The calculations are performed on periodically repeated slabs with three Cu, four O, and three Mg layers. The Cu layers contain  $7 \times 7$  atoms and the Mg and O layers contain  $6 \times 6$  atoms within the unit cell [8]. The slabs are separated by a "vacuum" layer of width 6.2 Å. In the starting configuration, the 147 Cu and 252 MgO atoms are placed in perfect lattice positions based on lattice constants  $a = 3.6(4.2)$  Å for Cu (MgO). The starting interface separation is 1.5 Å. The terminating layer of the MgO slab is chosen to be O, in accordance with experimental observation [5,9]. The Mg-terminated interface is known from coherent-interface calculations [10] to have smaller adhesive energy than the O-terminated interface. An unequal number of Mg and O layers is employed to avoid the spurious dipole moments and electric fields that occur for a stoichiometric cell [11]; the atomic structure close to the interface, however, would be similar if calculated with an equal number of Mg and O layers.

We employ the parallel plane wave pseudopotential code FEMD [12], in which the Kohn-Sham-Mermin states are self-consistently computed by iterative diagonalization and density-mixing methods. To minimize the numerical effort, orbitals only at the  $\Gamma$  point are calculated, and optimized pseudopotentials [13] with an energy cutoff of 47 Ry are employed. The large dimensions of the supercell ensure that an effective convergence is achieved with respect to  $k$ -point sampling. The internal atomic coordinates are relaxed to equilibrium based on calculated Hellmann-Feynman forces obtained from the self-consistent electron orbitals. After several dozen relaxation steps, the energy is converged to about  $10^{-3}$  eV/atom.

Figure 1 shows the relaxed atomic positions in the Cu and O layers adjacent to the interface, projected on the

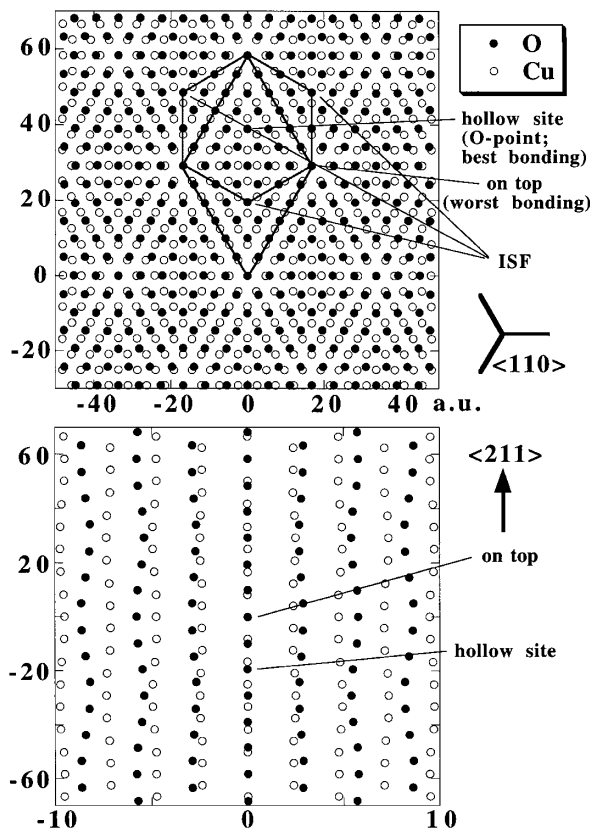


FIG. 1. Atomic positions in O and Cu layers adjacent to  $\{222\}$ MgO/Cu interface, projected onto the plane of interface. In the top panel, ordinate and abscissa scales are the same, whereas the abscissa scale is expanded and the ordinate scale is contracted in the bottom panel. Note the curvature of the atomic strings along the  $\langle 211 \rangle$  axis, which enables atoms to improve their bonding across the interface.

plane of the interface. The interface regions of strongest bonding are those where an atom on one side is nearly equidistant from three neighbors on the other side of the interface (threefold hollow sites); bridge sites coordinated to two neighbors across the interface are less favorable, and on-top sites are least favorable [10]. The points labeled ISF denote intrinsic-stacking-fault nodes. The planar stacking at these points is  $ABC/bca$  (rather than  $ABC/abc$ ), where the upper (lower) case characters refer to the stacking sequence on the metal (ceramic) side of the interface. The inscribed diamond indicates the size of the computational unit cell.

The relaxation (relative to perfect crystals) is not easily visible in the top panel of Fig. 1. By expanding the abscissa and compressing the ordinate axis in the lower panel, the curvature of the atomic strings in  $\langle 211 \rangle$  directions becomes evident. The curvature occurs because atoms relax locally to configurations that are more hollowlike and therefore more strongly bonded.

Relaxation also occurs perpendicular to the interface. The abscissa in Fig. 2 shows the mean value of the coordinate perpendicular to the interface for each atomic layer

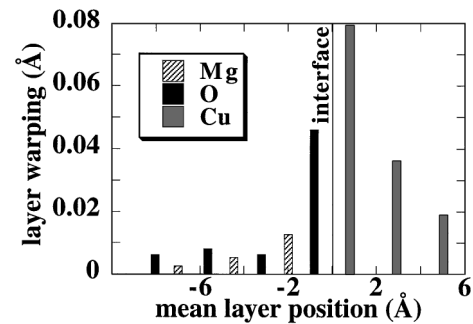


FIG. 2. Layer warping for  $\{222\}$ MgO/Cu defined as variance of the atomic coordinate perpendicular to the interface. The mean position of the layers relative to the interface at the origin is plotted on the abscissa.

and the ordinate is the variance of that coordinate, which is a measure of the layer puckering (or warping). It is often assumed that warping and relaxation in general are confined to the elastically softer metallic side of the interface [14]. The results in Fig. 2 are reasonably consistent with this assumption, with the significant exception of the interface O layer, whose warping is more than half that of the interface Cu layer. The absolute value of this warping, even for the interface Cu layer, is perhaps still too small to be observed by HREM. The warping occurs because the interface atoms that are approximately in hollow-site coordinations with respect to their neighbors across the interface are closer to the interface plane (at  $z = 0$  in Fig. 1) than atoms that are essentially in on-top configurations.

The adhesive energy is a measure of the strength of interface bonding. To estimate the adhesive energy for the semicoherent  $\{222\}$ MgO/Cu interface, we subtract the energies calculated for reference cells similar to that used for the interface except that all of the Cu atoms or all of the MgO atoms are removed. As in the interface calculation, all atoms are allowed to relax. The resultant adhesive energy is  $W = 3.6(2.7)$  eV per interface O (Cu) atom. A comparison with the result  $W = 3.1$  eV per interface atom for a coherent interface (calculated as described in previous work [15], but with different pseudopotentials) indicates these numbers are in the range expected. The difference between the results for a coherent interface and the present result for a semicoherent interface arise from the misfit and the atomic relaxation, both of which are omitted in the coherent case. These energies are relatively large compared to typical adhesive energies of less than an eV for neutral ceramic interfaces such as [6]  $\{100\}$ MgO/Ag or [15]  $\{100\}$ MgO/Cu. The mean interface spacing, i.e., the separation between mean layer positions on either side of the origin in Fig. 2, is  $1.6 \text{ \AA}$ , which is larger than that for the coherent interface ( $1.3 \text{ \AA}$ ). In the latter all interface atoms are in hollow-site configurations but in the semicoherent interface several atoms have on-top as well as hollow configurations, and arrangements in between. The bond length across the interface for atoms in the on-top configuration

is about 1.9 Å. This is close to the value of 1.8 Å obtained in coherent interface calculations [10], in which all interface atoms are in on-top positions.

Surfaces of constant pseudoelectron density are depicted in Fig. 3. The vertical axis in the figure is perpendicular to the interface. The doughnut-shaped objects represent interface Cu atoms. The plot illustrates the disparate bonding environments at the interface. The pair of atoms closest to the viewer are in an on-top configuration and the isodensity surfaces overlap extensively. In the regions of hollow-site and bridge-site configurations, the isodensity surfaces of Cu and O atoms on opposite sides of the interface are nonoverlapping. The on-top pairs experience overlap repulsion [10].

The standard analysis of semicoherent heterophase interface structure is in terms of misfit dislocations [2,16]. Interface properties, such as adhesive energy, can be represented in terms of properties of the ideal coherent interface, corrected for the effect of the dislocation network [17]. This framework, however, may not be the most appropriate when adjacent dislocation cores almost overlap. We consider here another type of structural analysis in which each atom in the interface layers of {222}MgO/Cu is assigned approximately to one of the three symmetry types, namely, hollow, bridge or on-top coordination, according to their local bonding across the interface. By inspection of Fig. 1, we find that of the 36 oxygen atoms in the interface unit cell, there are roughly 20 hollow-site, 9 bridge, and 7 on-top atoms, whereas of the 49 Cu atoms there are 30, 12, and 7 atoms in the three categories.

Since local patches of the semicoherent interface exhibit interface bond lengths similar to those obtained in corresponding coherent interface calculations [10], it appears reasonable to regard properties of the semicoherent interface roughly as weighted averages of properties of symmetric coherent interfaces (hollow site, bridge site, and on-top site). In previous work [5], the spatially resolved

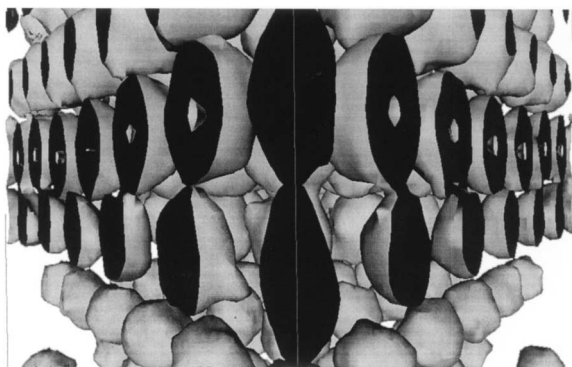


FIG. 3. Surfaces of constant pseudoelectron density in the vicinity of the interface. Doughnut-shaped objects represent Cu atoms. The vertical edge of the box is perpendicular to the interface. The Cu-O atom pair in the middle of the figure are in an on-top configuration and have overlapping isodensity surfaces, unlike those for bridge and hollow-site configurations.

EELS spectra at an MgO/Cu interface were interpreted in terms of coherent interface calculations for the hollow site [5,10]. In Fig. 4 are shown projected interface-layer densities of electronic states calculated for three different coherent interfaces and for bulk Cu and MgO. Details of the calculation are similar to those described in previous work [10]. These coherent-interface calculations provide higher resolution than the alternative procedure of projecting local densities of states at hollow site, bridge site, and on-top interface atoms in the 399-atom cell. With reference to the hollow-site panels in Fig. 4, we previously identified the feature within the MgO gap, in the region just below and just above the Fermi energy, as metal-induced gap states (MIGS) [5]. The EELS measurements of the O *K*-edge show a prepeak (below the bulk spectra) in the interface spectra that results from the unoccupied region of MIGS. We observe in Fig. 4 that the spectra for the bridge and on-top sites are shifted relative to those for the hollow site. In particular, the unoccupied densities of states are considerably greater for the on-top atoms than for the hollow site. Therefore the prepeaks in the O *K*-edge EELS spectra are sensitive to the on-top atoms, even though they are outnumbered by bridge and hollow-site atoms. The O(2*s*) semicore band at about -16 eV is also considerably shifted relative to that for the hollow-site configuration, which suggests that the interface dipole potential is significantly different.

In summary, this Letter presents a first principles calculation of the relaxed atomic structure of a ceramic/metal interface with the lattice mismatch included. The interface O and Cu layers both warp in such a way that the local interface spacing is largest in regions around on-top atoms, and smallest in the vicinity of the almost coherent hollow-site patches. The results suggest that equilibrium interface properties can be analyzed qualitatively as

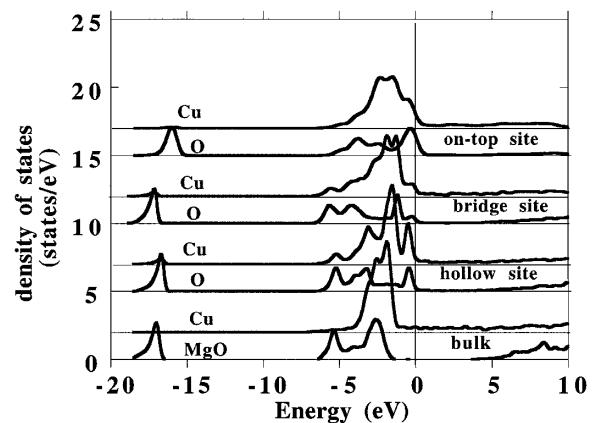


FIG. 4. Layer-projected density of electronic states for a {222}MgO/Cu interface. Spectra for the “bulk” are shown along with those for hollow site, bridge site, and on-top sites, for which interface separations are 1.3, 1.3, and 1.8 Å, respectively [10]. The zero on the abscissa scale corresponds to the Fermi energy. Gaussian broadening of 0.27 Å was employed.

weighted averages of properties of coherent interfaces for hollow-site, bridge-site, and on-top configurations. Calculations for coherent interfaces show that the electronic spectra in the MgO gap region, associated with MIGS, shift appreciably for on-top and bridge-site configurations relative to that for the hollow-site configuration.

R.B. and D.N.S. were supported at Northwestern University by the U.S. Department of Energy Grant No. DEFG02-96ER45597. L.H.Y. was supported at Lawrence Livermore National Laboratory by the U.S. Department of Energy under Contract No. W-7405-ENG-48. C.W. was supported by the Air Force Office of Scientific Research under Contract No. F33615-96-C-5258. This work was supported in part by grants of HPC time at the DoD Naval Oceanographic Supercomputer Center and the Army High Performance Computing Research Center.

---

\*Also at Materials Research Division, UES Inc., 4401 Dayton-Xenia Road, Dayton, OH 45432.

- [1] M. Rühle, *J. Surf. Anal. (Japan)* **3**, 157 (1997).
- [2] H.B. Groen, B.J. Kooi, W.P. Vellinga, and J.Th.M. De Hosson, *Philos. Mag. A* **79**, 2083 (1999).
- [3] D.A. Shashkov, M. Chisholm, and D.N. Seidman, *Acta Mater.* **47**, 3939 (1999); **47**, 3953 (1999).
- [4] D.K. Chan, D.N. Seidman, and K.L. Merkle, *Phys. Rev. Lett.* **75**, 1118 (1995).
- [5] D.A. Muller, D.A. Shashkov, R. Benedek, L.H. Yang, J. Silcox, and D.N. Seidman, *Phys. Rev. Lett.* **80**, 4741 (1998); *Mater. Sci. Forum* **294–296**, 99 (1999).
- [6] J. Purton, S.C. Parker, and D.W. Bullett, *J. Phys. Condens. Matter* **9**, 5709 (1997); J.A. Purton, D.M. Bird, S.C. Parker, and D.W. Bullett, *J. Chem. Phys.* **110**, 8090 (1999).
- [7] A calculation for a semiconductor heterophase interface has recently appeared [N. Oyama *et al.*, *Surf. Sci.* **435**, 900 (1999)].
- [8] In previous work [10], calculations were performed for a cell with  $a_{\text{MgO}}/a_{\text{Cu}} = 5/4$ , in which, in effect, both the MgO and the Cu were under strain parallel to the interface. The interface relaxation was somewhat similar to that obtained in the present work.
- [9] H. Jang, D.N. Seidman, and K.L. Merkle, *Interface Sci.* **1**, 61 (1993).
- [10] R. Benedek, D.N. Seidman, M. Minkoff, L.H. Yang, and A. Alavi, *Phys. Rev. B* **60**, 16094 (1999).
- [11] A. Pojani, F. Finocchi, J. Goniakowski, and C. Noguera, *Surf. Sci. B* **54**, 7697 (1997).
- [12] A. Alavi *et al.*, *Phys. Rev. Lett.* **73**, 2599 (1994). The FEMD code was built from CPMD V3.0, developed by J. Hutter *et al.* at IBM Research 1990–1996.
- [13] J.S. Lin, A. Qteish, M.C. Payne, and V. Heine, *Phys. Rev. B* **47**, 4174 (1993).
- [14] V. Vitek, G. Gutekunst, J. Mayer, and M. Rühle, *Philos. Mag. A* **71**, 1291 (1995).
- [15] R. Benedek, M. Minkoff, and L.H. Yang, *Phys. Rev. B* **54**, 7697 (1996).
- [16] F. Ernst, *Philos. Mag. A* **68**, 1251 (1993).
- [17] T. Hong, J.R. Smith, and D.J. Srolovitz, *J. Adhes. Sci. Technol.* **8**, 837 (1994).